

Perspective Article

Overload arthrosis: strain patterns in the equine metacarpal condyle

R.W. Norrdin¹, B.K. Bay², M.J. Drews², R.B. Martin², S.M. Stover³

¹Department of Pathology, College of Veterinary Medicine and Biomedical Sciences, Colorado State University, Fort Collins

²Orthopaedic Research Laboratories, University of California Davis Health Sciences Center, Sacramento

³J.D. Wheat Veterinary Orthopaedic Research Laboratory, School of Veterinary Medicine, University of California, Davis, USA

Abstract

An overload arthrosis occurs consistently in the palmar region of the metacarpal condyle of the equine fetlock (metacarpophalangeal) joint characterized by subchondral bone sclerosis, devitalization and mechanical failure leading to collapse of the overlying articular cartilage. Samples were selected of joints with mild, moderate, and severe subchondral sclerosis, in which cartilage collapse had not yet occurred. An additional group that had severe sclerosis with focal rarefaction suggesting impending collapse was also studied (n=5/group). Parasagittal slices were milled to 2.0 mm thickness and subjected to palmar forces 50 to 200% of those applied by the sesamoid bone at angles corresponding to early, mid and late stance support phases of the gait cycle. From contact radiographs in the loaded and unloaded samples, strains were determined by recognizing displacements in the trabecular patterns using texture correlation analysis. Failure did not occur in any of the samples. Strains were generally proportional to the forces applied and greatest at midstance. Strain patterns varied between samples and with the different loading positions. With increased subchondral bone sclerosis there was greater shear strain in overlying trabeculae. Strain patterns were not consistently different within the sclerotic bone at the site of failure. Focally higher strains at the surface were sometimes related to the edge of the platen which was molded to mimic the sesamoid bone in vivo. These results indicate that sclerotic thickening of subchondral bone transmits stresses to overlying trabeculae. No consistent strain pattern was recognized where devitalization and mechanical failure occurs. Focally higher strains related to the edge of the opposing sesamoid bone may play a role.

Keywords: Overload Arthrosis, Mechanical, Strain, Condyle, Subchondral Bone, Sclerosis

Introduction

Equine athletes are thought to develop unusually high stresses on joints during training and racing as juveniles and young adults¹. In the palmar metacarpal condyle of the fetlock joint, an overload arthrosis often occurs. The early or mild lesion is very common and asymptomatic but the severe changes are associated with fetlock lameness². The lesion is characterized by subchondral trabecular bone thickening (sclerosis) and sometimes devitalization and mechanical failure of the bone leading to collapse of the overlying articular cartilage^{1,3}. The lesion with cartilage infolding or collapse has been referred to clinically as "traumatic

osteochondrosis"¹. The failure occurs consistently in the sclerotic bone beneath the palmar articular surface that interfaces with the proximal sesamoid bones. There is thinning of the calcified cartilage⁴, and trabecular microfractures can be found histologically in the subjacent bone³. Differences in apparent density relative to adjacent bone could be responsible for the development of failure planes and such differences have been demonstrated at the site^{5,6}. In addition, the more perpendicular arrangement of the trabecular collagen suggested compressive forces from the sesamoid bones during the gait cycle were important in the adaptive response at the site³.

Recently, technology has become available to measure strain patterns in trabecular bone^{7,8}. The objective of the present study was to apply this technology to slices of the metacarpal condyle under compression to determine whether strain patterns such as focally higher strains, explained the predisposition of the site to failure.

Corresponding author: Robert W. Norrdin, Department of Pathology, CVMB, Colorado State University, Fort Collins, CO 80524, USA. E-mail: robert.norrdin@colostate.edu

Accepted 1 May 2001

Materials and methods

Metacarpal condyles used in this study were from a collection gathered in routine necropsies of Thoroughbred racehorses that had been training, racing or were involved in accidents at the time of death or euthanasia. Condyles (without the first phalanx or proximal sesamoid bones) had been stored in 70% alcohol. Contact radiographs of 2-3 mm thick parasagittal slices taken through the middle of the lateral condyle were available for selection of joints with mild, moderate, and severe subchondral sclerosis, in which cartilage collapse and "traumatic osteochondrosis" had not yet occurred. Severity of sclerosis was based on the area and radiodensity of bone in the palmar metacarpal region. An additional group that had severe sclerosis, in which an area of focal radiolucency or rarefaction suggested impending collapse was also studied and designated severe+rarefaction. There were five animals in each group. The total of 20 condyles were from horses ranging in age from two to six years. Nine were from females and eleven from males, including four geldings.

Parasagittal slices lateral to those used for radiographs were cryomilled to 2.0 mm thickness, potted with polymethylmethacrylate (Coe TrayPlastic, GC America Inc., Alsip, IL 60803) in a tray and loaded in a customized jig mounted within a contact radiography unit (Faxitron X-Ray Corp., Buffalo Grove, IL) as previously described⁸. The samples were loaded against a stationary polymethylmethacrylate platen molded to the form of the articulating sesamoid bone surface. The angles and position of the sesamoid bone-shaped platens on the condylar surface were copied from radiographs of the normal equine limb (Fig. 1) used to determine range of motion⁹ for the construction of a three-dimensional model of the musculoskeletal geometry¹⁰. A polymethylmethacrylate platen molded to the articular surface had to be poured for each sample and for two of the three gait phases. Samples were subjected to palmar forces that were 50 to 200% of those applied by the sesamoid bone at angles corresponding to early, mid and late stance support

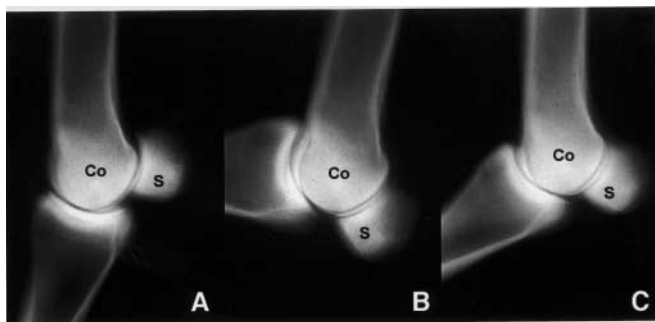


Figure 1. Lateral radiographs of a normal equine limb (*ex vivo*) during early (A), mid (B), and late (C) stance phases of the gait cycle (Zarucco et al., 1997). These were used to determine the angle and position of the sesamoid bone (S) during loading of the metacarpal condyle (Co) to evaluate strain patterns.

phases of the gait cycle. The forces were calculated for an average animal of 500 Kg body weight using forces at a gallop from the literature and a model of stress vectors in the fetlock joint¹¹ to estimate load applied by the sesamoid bone. The base load was normalized for size from measurements of the diameter of the condyle. This was done by multiplying the base load by the ratio of the diameter of the specific condyle to the average condyle diameter for all samples. The total width of the weight-bearing surface of the condyles was measured and the total force on that condyle multiplied by the fraction of total condyle width represented by the 2 mm thickness of the parasagittal slice being tested. For early stance, there was an angle of 110 degrees between the shaft of the metacarpal bone and the sesamoid. At midstance, where forces are highest, there was an angle of 140 degrees and at late stance, there was an angle of 115 degrees. Forces used were 50% to 200% of calculated load and actual maximum loads were 320-370N at early stance, 640-760N at midstance, and 580-645N at late stance. Maximum loads at each stance phase were generally used in statistical evaluation of the strain data. From contact radiographs (Industrex M film, Eastman Kodak Company, Rochester N.Y.) in the loaded and unloaded samples, digitized images were compared and strains in the condyle were determined using texture correlation analysis⁷. This is done with a specialized computer program using a pattern matching algorithm in overlain images to recognize displacements in the trabecular patterns. Strains are calculated from the measured displacement fields by a numerical differentiation procedure. Since this method depends on adequate contrast to outline bone structure and works best in trabecular bone, readings were not consistently obtained in areas of sclerosis where there was little difference in gray scale. In a subsequent study with three animals each from the mild, severe and severe+rarefaction groups, speckling of the sclerotic zone with lead powder was used to study this area specifically and compare it to the trabecular bone in the rest of the condyle. This was accomplished by applying a thin layer of cyanoacrylate glue (Loctite 416, Loctite Corp., Rocky Hill, CT 06067) to the sclerotic region and sprinkling it with fine lead powder (Pb100-325 mesh, Atlantic Equipment Engineers, Bergenfield NJ). This technique has been used successfully previously¹².

Qualitative evaluation was done by comparing radiographic images with strain patterns looking for consistencies in the pattern at different loads and stance phases. Data were generally evaluated as maximum shear strain, i.e., strain at those sites where the interface of strains in all directions produced the greatest shear. The texture correlation technique generates the entire strain tensor, therefore any strain invariant can be derived and analyzed. For this study we focused on maximum shear strain, which is the highest magnitude shear strain that exists at any particular location within the sample, regardless of the principal strain directions. Failure in many materials, including bone, is sensitive to shear strains⁸.

Consistent with previous studies on strains within

trabecular bone samples¹³, this study found strain populations that were highly non-normal. Means and standard deviations calculated directly from these data sets do not accurately reflect data central tendency and dispersion. More meaningful measures were derived by using a nonparametric, percentile-based approach. Low, mid and high range values were calculated as the 17th, 50th, and 83rd percentiles, respectively, of the ordered data. These values are comparable to the mean \pm one standard deviation calculated from normally distributed data¹³. Groups with various degrees of sclerosis were compared statistically by analysis of variance using these three range values as continuous variables.

In comparing strain in the sclerotic and trabecular regions in the lead-speckled subgroups, the sclerotic area was outlined in an image analysis program (NIH Image) and the values were determined directly from gray scale values for mean and maximum in the contour plots of maximum shear strain. Analysis of variance, with these as continuous variables, was used to look for an effect of sclerotic vs trabecular location. Fisher's least significant difference test was used to look for significant differences in these variables for each of the sclerotic and trabecular regions, between mild, severe and severe+rarefaction groups.

Results

Obvious failure did not occur during mechanical testing in any of the samples with the forces applied. However, in one animal from the group with severe sclerosis and focal rarefaction, a fracture line was already present in the area of focal rarefaction (Fig. 2). In the radiographs of slices used for loading there were some differences in the proportion of sclerotic bone within the condyle as compared to the original radiographs used for selection of the groups which were more medial on the condyle. This was most apparent in the mild and moderate groups where there was considerable overlap and little distinction between the groups.

Strains were generally proportional to the forces applied and greatest at mid stance. In qualitative observations, strains

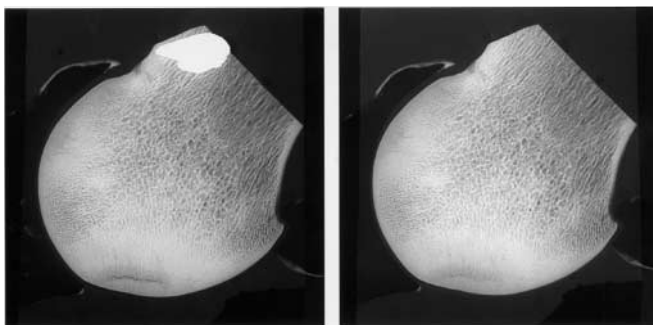


Figure 2. Radiograph of unloaded (left) and loaded (right) metacarpal condyle from the group with severe sclerosis and focal rarefaction. In this sample a linear fracture can be seen in the area of focal rarefaction in the unloaded sample at left. It is closed upon loading at right. This was the only fracture line seen.

in the same condyle had similar contour patterns as strains increased with higher loads (Fig. 3). There was considerable variation, however, between samples and little consistency at the palmar surface (see Figs. 3 and 5b,c). Strains were generally lower throughout the sclerotic subchondral region and higher in the overlying trabeculae in the middle and proximal parts of the condyle (Fig. 5b,c). The trabeculae at the proximal palmar subchondral area also had higher strains. The latter was more pronounced with the more acute angle of loading and slightly more proximal position of the platen in the early and late stance loading positions. In the subchondral area, variable localized areas of high strain were not consistently correlated with radiographic bone patterns within the limitations of resolution available. Some foci may have represented edge effects at the margin of the platen which had been shaped to mimic the sesamoid bone *in vivo*. These were seen in only a small number of tests and not in any specific group.

In the plots of shear strain, focal blank areas of off-scale readings were seen in areas where there was inadequate trabecular pattern (Fig. 3) and four samples were excluded from the statistical evaluation because these areas were too extensive (greater than 35-40%). Statistically, samples with severe subchondral bone sclerosis tended to develop greater shear strain in the condyle. This was significant when the mild and moderate groups were combined and compared to the combined severe groups (Fig. 4). In the group with severe sclerosis and focal rarefaction, there were somewhat lower values (not significant) than in the severe group, suggesting there had been partial reduction of the stresses.

In the lead-speckled subgroups used to better evaluate the sclerotic area (Fig. 5), there were more complete plots of the sclerotic area but patterns were generally similar to those in

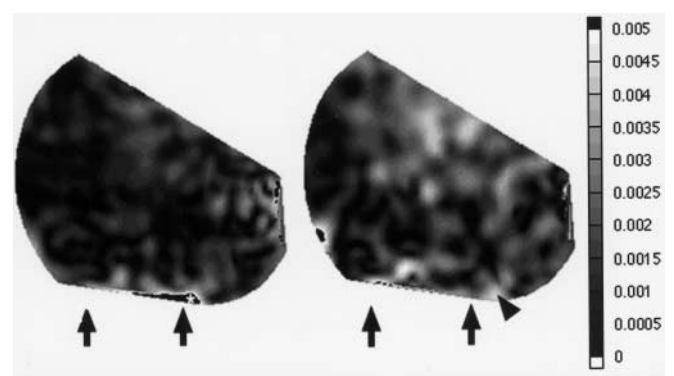


Figure 3. Contour plot of maximum shear strain in a condyle loaded with 300 (left) and 600 (right) Newtons in the midstance position. Arrows at bottom show the direction of loading and strain values are given in scale at right. There was general consistency in strain patterns with greater strains at higher loads within the same samples. Areas of higher strain in the subchondral sclerotic region (arrowhead at right) were seen in some samples and sometimes could be related to the edge of the sesamoid-like platen. Small dark areas (see asterisk at left) usually represented off-scale gaps in the plots due to lack of radiographic contrast in the more sclerotic (radiodense) areas.

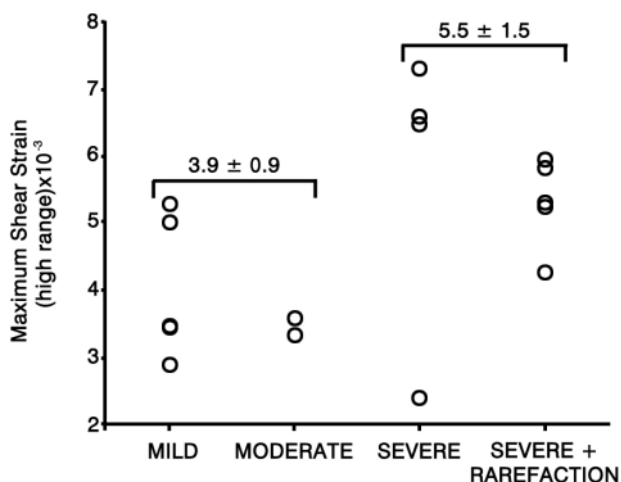


Figure 4. Plot of maximum shear strain (high range values) in the condyles as a whole. When mild and moderate groups were combined and compared to combined severe groups, higher values were seen in the latter ($P < 0.05$).

the whole condyle. There was often little or no strain seen in the sclerotic area. No consistent change was seen in the rarefied zones within the sclerotic area in the three samples studied. In the sample that already had a trabecular fracture there was an off scale gap in the region at the higher load levels.

On statistical evaluation of the lead-speckled subgroups comparing the sclerotic zone with overlying trabeculae, maximum values for shear strain were higher in the trabeculae than in the sclerotic area and the difference was significant at all stance phases (Fig. 6). Mean values for shear strain were significantly different at the mid and late stance phase. Within the lead-speckled subgroups, there was no difference between the mild, severe, and severe+ rarefaction groups in strain levels in either the sclerotic or trabecular zone.

Discussion

The purpose of this study was to determine strain patterns under compression, in the condyles of racehorses that had mild, moderate and severe subchondral bone sclerosis as a result of presumed overload arthrosis. This was done to determine whether there were consistent patterns, such as focally higher strains, in the palmar subchondral bone that explain mechanical failure at the site. Testing was done on slices of the condyle which were presumed to be representative of the intact condyle at that site. In addition, since only the condyles were available for testing, a polymethylmethacrylate platen molded to the form of the opposing sesamoid bone had to be used in its place. Studies comparing this material to natural bone and intervertebral joint found it produced more homogeneous strains which were less like the physiological state¹³. Within these constraints however, the results are considered generally indicative of strains in the condyle with increasing degrees of subchondral sclerosis.

The results indicate that surface forces are transmitted throughout the condyle. There were generally higher strains in the trabecular bone in the middle of the condyle than in the more dense subchondral bone. Strain patterns were generally consistent in the same sample at each loading position and strains increased with increasing load. There was however, variation between samples at each loading position. There was also variation within samples as the loading angle and contact surface were changed to mimic different phases of the gait cycle. Generally, loading more proximally on the palmar condyle to mimic early and late phases resulted in higher strains in the proximal palmar trabeculae where there is less dense subchondral bone. At midstance, forces were applied more directly over the region of subchondral sclerosis and strains were higher in the

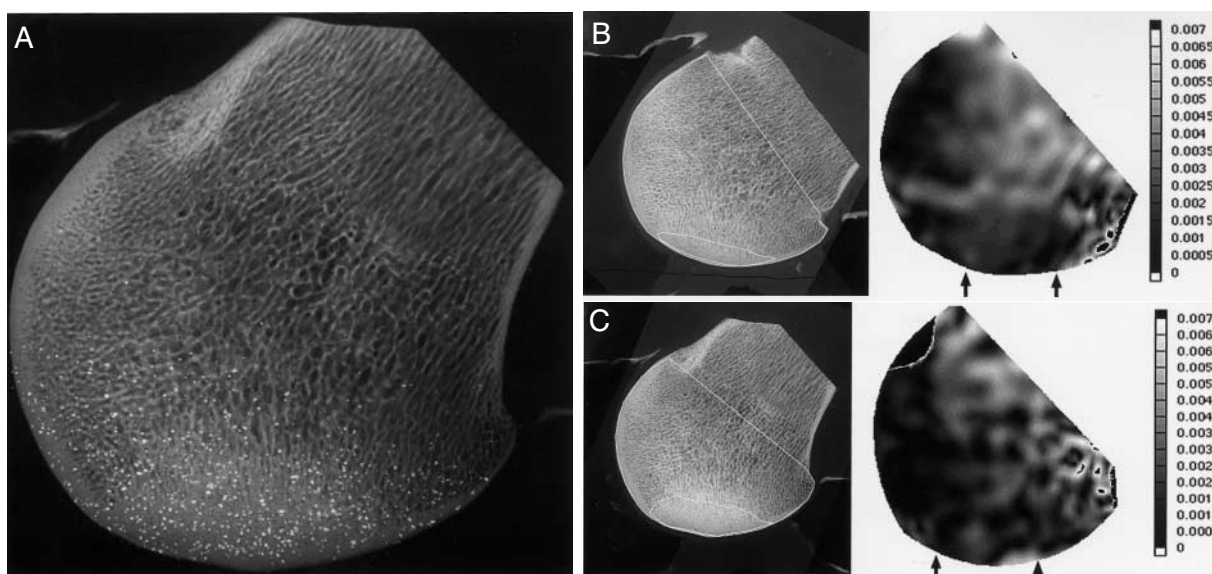


Figure 5. Lead speckling of more radiodense areas (A) was used to obtain more complete strain plots of the sclerotic zones as outlined in two different samples in B and C. The generally lower strains in the sclerotic zones and variation in patterns between samples can be seen.

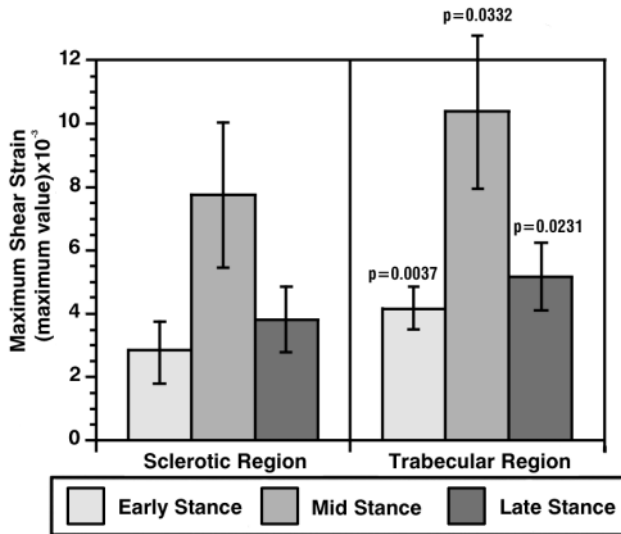


Figure 6. Plot of maximum shear strain (maximum values) in sclerotic and trabecular regions of lead-speckled groups at early, mid and late stance positions. Highest strains were seen at midstance where loads were greatest. Strains were higher in the trabecular region at all stance phases (P value is given).

trabeculae in the middle and more proximal regions of the condyle. Strains were not analyzed beyond a line drawn across the proximal end of the condyle but presumably continued into the metaphyseal trabeculae. This has been found in other model systems¹⁴. In comparing shear strains in animals with mild and moderate subchondral sclerosis to those with severe sclerosis and severe sclerosis with focal rarefaction, higher mean maximum shear strains were seen in samples with severe sclerosis. This indicates that an increasing amount of stiffer sclerotic subchondral bone transmits greater strain to the overlying trabeculae.

In the subchondral bone itself, the lack of contrast in the sclerotic zone frequently led to off-scale readings and gaps in the strain plots. This was improved by speckling this region with a lead powder. These readings were more complete but the strain patterns throughout the condyle were generally similar to those in the original unspeckled samples. No consistent pattern was seen within the sclerotic region. By outlining the sclerotic region and comparing strain values to the rest of the condyle, significantly greater strains were found in the overlying trabeculae. Values in the sclerotic region were approximately 60-70% of those in the trabecular region at the higher load levels. Some focal strain variations could be seen in the sclerotic area adjacent to the palmar surface, but these were not consistent, nor were they frequent in the area where failure would be expected. In a few cases, focally higher strains appeared to correspond to the edge of the platen but this was not consistent. Such an edge effect could also be important *in vivo* however, since the site of failure often corresponds to the distal edge of the proximal sesamoid bone³.

In the samples with severe sclerosis and focal rarefaction there was no consistent change in the strain pattern that

corresponded to the focal rarefaction. If these foci are areas of activated remodeling in which resorption has decreased radiodensity of the sclerotic subchondral bone, greater strains might be expected at the site. The sensitivity of our methodology may not have been sufficient to detect these strain differences. Fractures adjacent to areas of increased density have been seen at the palmar site, both radiographically and with scanning electron microscopy^{5,6}. In the one sample from this group in which a fracture line was seen in the radiographs, there were off-scale readings at higher load levels which indicate gross displacement at the site. The closing of the fracture line upon loading could actually be seen in the sequential radiographs (Fig. 2). This horse had a sagittal fracture of the contralateral metacarpal condyle which was no doubt responsible for its euthanasia. Whether the transverse fracture line developed acutely or had been subclinically present for a period of time is not known. An association of longitudinal condylar fractures with defects in the contralateral limb has been previously reported as evidence for pre-existing microdamage⁶.

In summary, these studies have shown that compressive forces applied at the articular surface produced strains throughout the condyle. The pattern varied with the angle and contact site corresponding to different phases of the gait cycle. The strains were higher with increasing load and highest at mid stance of the equine gait cycle. With increased severity of subchondral bone sclerosis there tended to be greater transfer of strains to the less stiff overlying trabeculae. There was significantly greater strain in the trabecular region compared to the sclerotic region of the condyle. Within the sclerotic subchondral bone no consistent pattern was seen at the site where bone failure is known to occur. Focally higher surface strains were sometimes associated with the edges of the platen which was molded to mimic the position of the sesamoid bone *in vivo*. This may indicate that a more complex mixture of forces than simple direct compression is important in producing focal subchondral bone damage in arthrosis.

Acknowledgements

This study was funded by grant #98 EQ-29 from the Morris Animal Foundation. The authors gratefully acknowledge the contribution of the condyle specimens and collection of historical data by Dr. Derek Read and colleagues, California State Veterinary Diagnostic Laboratory at San Bernardino, and Dr. Bill Johnson, California State Veterinary Diagnostic Laboratory at Davis.

References

1. Pool RR, Meagher DM. Pathologic findings and pathogenesis of racetrack injuries. *Vet Clinics No Amer (Equine Pract)* 1990; 6:1-30.
2. Hornoff WJ, O'Brien TR, Pool RR. Osteochondritis dissecans of the distal metacarpus in the adult racing Thoroughbred horse. *Vet Radiol* 1981; 22:98-106.
3. Norrdin RW, Kawcak CE, Capwell BA, McIlwraith CW. Subchondral bone failure in an equine model of

- overload arthrosis. *Bone* 1998; 22:133-139.
4. Norrdin RW, Capwell BA, Kawcak CE, McIlwraith CW. Calcified cartilage morphometry and its relationship to subchondral bone remodeling. *Bone* 1999a; 24:109-114.
 5. Riggs CM, Whitehouse GH, Boyde A. Pathology of the distal condyles of the third metacarpal and metatarsal bones of the horse. *Eq Vet J* 1999; 31:140-148.
 6. Stover S, Read D, Johnson B, Harrington T, Ardans A, Anderson A, Barr ML, Daft BC, Kinde H, Moore J, Stolz J, Woods LW. Lateral condylar fracture histomorphology in racehorses. *Proc Am Assoc Equine Pract* 1994; 40:173.
 7. Bay BK. Texture correlation: a method for the measurement of detailed strain distributions within trabecular bone. *J Orthop Res* 1995; 13:258-267.
 8. Bay BK, Yerby SA, McLain RF, Toh E. Measurement of strain distributions within vertebral body sections by texture correlation. *Spine* 1999; 24:10-17.
 9. Zarucco LP, Swanstrom M, Stover SM, Hubbard M, Wisner E. *In vitro* assessment of the instant centers and angles of rotation of the equine Thoroughbred forelimb joints. Vet Orthop Soc 24th Ann Conference, Big Sky, Montana; March 1-8, 1997:p42.
 10. Zarucco LP, Swanstrom M, Stover SM, Hubbard M, Wisner E. Image processing and co-registration of CT and MRI images: 3-D musculoskeletal geometry reconstruction for equine forelimb computer model generation. Vet Orthop Soc 25th Ann Conference, Snowmass, CO; Feb 21-28, 1998:p56.
 11. Martin RB, Burr DB, Sharkey NA. *Skeletal Tissue Mechanics*. Springer-Verlag, New York; 1998:20-23.
 12. Russell SS, Sutton MA. Strain field analysis acquired through correlation of X-ray radiographs of a fiber-reinforced composite laminate. *Exp Mech* 1989; 29:237-240.
 13. Yerby SA, Bay BK, Toh E, McLain RF, Drews MJ. The effect of boundary conditions on experimentally measured trabecular strain in the thoracic spine. *J Biomech* 1998; 31:891-897.
 14. Van Rietbergen B, Muller R, Ulrich D, Ruegsegger P, Huiskes R. Tissue stresses and strain in trabeculae of a canine proximal femur can be quantified from computer reconstructions. *J Biomech* 1999; 32: 443-451.